Patterns of Neointima Formation after Coil or Stent Treatment in a Rat Saccular Sidewall Aneurysm Model.

Basil E. Grüter MD[1,2], Stefan Wanderer MD[1,2], Fabio Strange MD[1,2], Gwendoline Boillat MD[1,2], Dominik Täschler MSc[2], Jeannine Rey MD[2], Davide Croci MD[2], Denis Grandgirard PhD[3, 4], Stephen L. Leib Prof, MD[3, 4], Michael von Gunten MD[5], Stefano Di Santo PhD[4, 6], Hans Rudolf Widmer Prof, PhD[4,6], Luca Remonda Prof, MD[7], Lukas Andereggen MD[1,2], Edin Nevzati MD[1,2], Daniel Coluccia MD[1,2], Javier Fandino Prof, MD[1,2] and Serge Marbacher MD, PhD[1,2]

[1] Department of Neurosurgery, Kantonsspital Aarau, Switzerland

[2] Cerebrovascular Research Group, Department for BioMedical Research, University of Bern, Bern, Switzerland

[3] Neuroinfection Laboratory, Institute for Infectious Diseases, University of Bern, Bern, Switzerland

[4] Cluster for Regenerative Neuroscience, Department for BioMedical Research, University of Bern, Bern, Switzerland.

[5] Institute of Pathology Laenggasse, Ittigen, Switzerland

[6] Department of Neurosurgery, Bern University Hospital, Inselspital Bern, Bern, Switzerland

[7] Division of Neuroradiology, Department of Radiology, Kantonsspital Aarau, Switzerland

Correspondence to: Basil E. Grüter, MD; Department of Neurosurgery c/o NeuroResearch Office, Kantonsspital Aarau; Tellstrasse 1, 5001 Aarau, Switzerland, +41/ (0) 62 838 66 34, Fax: +41/ (0) 62 838 66 29; Email: basil.grueter@ksa.ch; neurosurgery@ksa.ch

Cover title: Aneurysm healing with endovascular treatments

Tables 0, Figures 6

Key words: Aneurysm; Endovascular treatment; Coil; Stent; Animal model

Subject terms: Aneurysm; Treatment; Stent; Animal Models of Human Disease; Basic Science Research

Manuscript: 3675 words; Total word count (including title page, references, and figure legends): 6273

Abstract

Background and Purpose: Endovascular aneurysm treatment relies on a biological process, including cell migration for thrombus organization and growth of a neointima. To better understand aneurysm healing, our study explores the origin of neointima-forming and thrombus-organizing cells in a rat saccular sidewall aneurysm model.

Methods: Saccular aneurysms were transplanted onto the abdominal aorta of male Lewis rats and endovascularly treated with coils (n = 28) or stents (n = 26). In 34 cases, green-fluorescent protein expressing (GFP+) vital aneurysms were sutured on wild-type rats and in 23 cases decellularized wild-type aneurysms were sutured on GFP+ rats. Follow-up at 3, 7, 14, 21, and 28 days evaluated aneurysms by fluorescence angiography, macroscopic inspection, and microscopy for healing and inflammation status. Furthermore, the origin of cells was tracked with fluorescence histology.

Results: In animals with successful functional healing, histological studies showed a gradually advancing thrombus organization over time characterized by progressively growing neointima from the periphery of the aneurysm toward the center. Cell counts revealed similar distributions of GFP+ cells for coil or stent treatment in the aneurysm wall (54.4% vs 48.7%) and inside the thrombus (20.5% vs 20.2%) but significantly more GFP+ cells in the neointima of coiled (27.2 %) than stented aneurysms (10.4%) ($p = 0.008$).

Conclusion: Neointima formation and thrombus organization are concurrent processes during aneurysm healing. Thrombus organizing cells originate predominantly in the parent artery. Neointima formation relies more on cell migration from the aneurysm wall in coiled aneurysms

but receives greater contributions from cells originating in the parent artery in stent-treated aneurysms. Cell migration, which allows for a continuous endothelial lining along the parent artery's lumen, may be a prerequisite for complete aneurysm healing after endovascular therapy. In terms of translation into clinical practice, these findings may explain the variability in achieving complete aneurysm healing after coil treatment and the improved healing rate in stent-assisted coiling.

Non-standard Abbreviations and Acronyms

EVT: Endovascular therapy

GFP: Green fluorescent protein

SMC: Smooth muscle cell

Introduction

With increasing popularity of endovascular therapy (EVT) as a primary treatment strategy for intracranial aneurysms during the past decades, the number of patients with aneurysm recurrence after coil treatment has increased. Depending on aneurysm characteristics (e.g., size, location, rupture status) and to some extent the technical nuances in EVT procedures, studies have reported up to 30% of patients develop aneurysm recurrence after coil treatment.[1, 2] Compared with a mechanical strategy like clipping that creates an immediate direct endothelium-endothelium contact under the former aneurysm orifice, EVT induces a biological healing process that consists of cell migration, thrombus organization, matrix synthetization, neointima formation, and eventually intraluminal aneurysm scar formation.[3]

Smooth muscle cells (SMC) play a fundamental role in that biological healing process after coiling.[4, 5] On one hand, clinical and preclinical studies revealed loss of mural cells was a relevant factor for aneurysm growth and rupture.[6, 7] On the other hand, experimental studies showed intra-aneurysmal transplantation of SMCs or systemic injection of mesenchymal stem cells (as single treatment or adjuvant to coiling) were factors in promoting complete aneurysm healing and preventing aneurysm growth and rupture.[8-10] As yet, the origin of SMCs that mediate aneurysm healing after endovascular treatment in a physiological setting remains unclear and controversial.[4, 11-14] However, this question is of paramount importance for the development of novel bioactive endovascular materials, cell-based therapies, or potential systemic drug therapies.

Toward a deeper understanding of these fundamentals, our study explores the origin of neointima-forming and thrombus-organizing cells in a rat saccular sidewall aneurysm model. We investigate the healing process, noting any differences between specific regions of interest in the aneurysm complex, specifically the aneurysm wall, intraluminal thrombus, and neointima. Finally, we compare aneurysm healing on a cellular level study between coil and stent treatments

in these regions. Toward the aim of translating our findings into clinical practice, we have discussed our experimental findings in this context when possible.

Methods

Ethics and Animals

The authors declare that all supporting data are available within the article and its online supplementary files. All experiments were approved by the Committee for Animal Care of the Canton Bern, Switzerland (BE 65/16) and reported in accordance with the ARRIVE guidelines.[15] Saccular sidewall aneurysms were microsurgically created in 57 male Lewis rats. All animals were housed in groups of 4 and received care in accordance with institutional guidelines. At the time of surgery, they were 12 weeks or older and weighed 488 ± 49 grams. Of these, 23 animals were transgene Lewis rats, expressing green-fluorescent protein (GFP+) in a mosaic pattern (LEW-Tg(CAG-EGFP)1Ys)[16] and 34 expressed a wild-type phenotype (controlled inbred in an international reference laboratory). For the experiments, GFP+ aneurysms were sutured on wild-type recipient animals and vice versa wild-type aneurysms were sutured on GFP+ recipients.

Study Design

Animals were randomly allocated to undergo either coil (n = 30) or stent (n = 27) treatment. An a priori sample size calculation to reach significance then targeted n > 8 animals per group, with an estimated difference of 20% between groups; accordingly, our study groups consisted of 9-10 animals. For each group, follow-up times were defined at 3 days, 7 days, 14 days, 21 days, and 28 days upon euthanasia, followed by harvesting of the aneurysm and its parent artery, and histologic processing. To ensure reproducibility**,** all specimens were analyzed and repeated at each timepoint (except for one single probe at 28 days with stent treatment). For

GFP+ aneurysms in wild-type animals, replication cohorts were performed with follow-up on 7 and 21 days. Study design shows drop-out rates and follow-up schedules in Figure 1. Primary endpoints were defined as the proportion (%) of GFP+ cells specific for one of three ROIs, specifically the aneurysm wall, intraluminal thrombus, or neointima. Secondary endpoints were defined as aneurysm healing by macroscopic inspection and fluorescence angiography, and histological analysis of neointima formation, aneurysm wall cellularity and inflammation, and periadventitial inflammation and fibrosis.

Anesthesia, Aneurysm Formation, and Treatment

General anesthesia was introduced by inhalation of isoflurane 4%, followed by an intraperitoneal injection of 0.5 mg/kg medetomidine (Medetor; Virbac, Switzerland) and 50 mg/kg ketamine hydrochloride (Ketalar; Pfizer, Switzerland). Subcutaneous injection of buprenorphine (0.3mg/kg, Temgesic; Indivior, Switzerland) was used for analgesia. The anesthesia protocol for the replication cohorts was revised as described in the Supplementary Methods. Our model used the methodology of the Helsinki rat aneurysm model and coil or stent treatment as described elsewhere.[5, 17, 18] Briefly, sidewall aneurysms were created by end-to-side anastomosis of a ligated arterial-vessel pouch from a donor animal (thoracic aorta) to the clamped abdominal aorta of a recipient animal. Wild-type aneurysms were incubated for 10 hours at 37°C in 0.1% sodium dodecyl sulfate (SDS) in Milli-Q water for decellularization of the vessel wall as previously described.[6] Coiling was performed immediately during aneurysm suturing, with the final quadrant still open, using 2 cm of a Target 360 TM Ultra coil (2mm/3mm diameter) (Stryker, Kalamazoo, MI, USA). Stenting included clipping of the abdominal aorta proximal to the aneurysm, punctuation of the aorta distal to the aneurysm, and then endovascular stent deployment in modified Seldinger technique. A modified Magmaris device (AMS with polymer

coating) of 6-mm length, 2.5-mm diameter, and nominal pressure of 8 bar, (Biotronik, Bülach, Switzerland) mounted on a baloon was used. A digital video camera (Sony NEX-5R, Sony, Tokyo, Japan) attached to a stereo microscope (OPMI, Carl Zeiss AG, Oberkochen, Germany) was used to document aneurysm dimensions preoperatively, at harvest, and during operative procedures.

Fluorescence Angiography, Macroscopic Inspection, and Tissue Preparation

Fluorescence angiography was performed in all cases to assess dynamic perfusion status after the intravenous injection of 2 ml fluorescein (fluorescein 10% Faure, 0.5 g/5 ml). Next, illumination (light source 465 to 490 nm) of the aneurysm was filmed with a specified detection filter as previously described.[19] After animals were euthanized with an overdose of intracardial ketamine hydrochloride (Narketan, 120 mg/kg ketamine injection, Vetoquinol, Switzerland), the aneurysms were harvested and measured in all dimensions, and the posterior aorta was opened to inspect the aneurysm orifice. Tissues were immediately fixed in formalin (4% weight/volume solution, J.T. Baker, Arnhem, The Netherlands) until paraffin embedding for histological analysis.

Histological Analysis

Paraffin-embedded aneurysms were cut in parallel to the underlying parent artery in 2-μm slices and visualized with hematoxylin-eosin (HE), Masson-Goldner trichrome (MASA), smooth muscle actin (SMA), and Von Willebrand factor (F8) staining. These stained slices were digitized (omnyx VL120, GE, USA) and evaluated with the JVS viewer (JVS view 1.2 full version, http://jvsmicroscope.uta.fi/software/, University of Tampere, Finland). All light microscopy underwent qualitative analysis by 2 observers using a 4-tier grading system[6] to rate neointima formation and

locoregional inflammation (see Supplementary Methods). For fluorescence microscopy, slides were cut into a 4 μm-thickness, deparaffined, and incubated with an anti-GFP antibody. Next, they were linked to a secondary fluorescent antibody to intensify the GFP signal (further detailed in the Supplementary Methods) and stained with DAPI. All slides were digitally photographed with a fluorescence microscope (Olympus BX51, Hamburg, Germany; Cell Sens Dimension Imaging software v1.8). Calculations of the proportion of GFP+ cells on all cells for the three ROIs were performed with a semi-automated cell count using image-J software (Image-J version 1.52n, U.S. National Institutes of Health, Bethesda, Maryland, USA, https://imagej.nih.gov/ij/).

Exclusion Criteria and Statistical Analysis

Exclusion from final analysis were premature death/euthanasia due to surgical morbidity/mortality in 3 animals (1 anesthesia intolerance, 1 with aneurysm growth and rupture 7 days after coiling, 1 with hemiparesis due to subacute aortic thrombosis 7 days after coiling) and inadequate post-processing of the specimen in 1 animal. To avoid bias, no cell counts inside the thrombus were done for specimens at 3-day follow up because no organized thrombus was yet present at that early stage of healing; with a negligible number of cells present inside the aneurysm sac, meaningful analysis was impossible. ANOVA test was used to compare cell counts between coil and stent treatments. Two-tailed Fisher exact test was used for comparison of dichotomized histological grades among all groups. Student t test was performed to assess differences in surgical characteristics and histological analyses between two groups. Data were analyzed and visualized using Graph Pad Prism 8 (Version 8.2.0.435, GraphPad software, San Diego, CA, USA). Values are expressed as mean ± standard deviation (SD) or median and interquartile range. A probability value < 0.05 was considered statistically significant and < 0.001 highly significant.

Results

Aneurysm Healing and Surgical Outcome

At follow up, stent-treated aneurysms showed a clear pattern of healing: within 3 days, a thin, but continuous, neointima had developed, separating the blood flow in the parent artery from the aneurysm dome (Figure 2). Within 21 to 28 days, progressive thrombus organization with extensive scarification had formed with only minor residual hematoma at the tip of the aneurysm. At follow-up, none of the stent-treated aneurysms showed aneurysm recurrence by means of fluorescence angiography. However, histology revealed central minor residual perfusion in 1/26 (4%) cases. In contrast, 16 (57%) of all 28 coiled aneurysms showed signs of residual aneurysm perfusion at follow-up especially among 7/10 (70%) of aneurysms with decellularized vessel walls (Supplementary Table I, status of aneurysm healing and growth). In general, growth of coiled aneurysms was more pronounced during the study period (Supplementary Figure I). For example, one coiled aneurysm enlarged to form a giant aneurysm; one animal whose aneurysm ruptured after 7 days was excluded from final analysis; and one animal developed hemiparesis due to subacute aortic thrombosis caused by a thrombus distal to the aneurysm.

There were no relevant differences between stent and coil treatment groups regarding animal characteristics such as age or body weight. Total operation time averaged longer for stenting (147 minutes ± 31 minutes) than coiling (92 minutes ± 29 minutes) because of the more complex setting; specifically, this included reperfusion time between aneurysm creation and re-clipping for stent introduction and the need for an additional microsuture at the puncture (stent insertion site). Other than that, no relevant differences were noted in the key procedural steps detailed in Supplementary Figure II.

Cell Count Comparison between Coil and Stent Treatment

Cell counts for the proportion of GFP+ cells in the aneurysm wall revealed no relevant difference between coil (49.2% ± 11.8%) and stent (48.7% ± 10.3%) treatment ($p = 0.37$). Cell counts showed no relevant differences in the proportion of GFP+ cells in the aneurysm wall between coil (49.2% ± 11.8%) and stent (48.7% ± 10.3%) treatments (p 0.37), or in the intraluminal thrombus between coil (20.5 % ± 8.3%) and stent (20.3% ± 5.9%) treatments (p 0.94). However, there were significantly more GFP+ cells in the neointima of coiled aneurysms (31.6% ± 11.0%) than in stent-treated aneurysms (8.4% ± 6.0%), $p<0.0001$ (Figure 3). The replicate cohort confirmed these observations between treatments. Specifically, findings showed no relevant differences between coils (46.3% ± 6.9%) and stents (49.0% ± 5.2%) in the aneurysm wall ($p = 0.47$) or between coils (24.0% ± 10.8%) and stents (27.4% ± 4.8%) in the thrombus ($p = 0.49$). However, significantly more GFP+ cells were found in the neointima of coiled aneurysm (29.1% ± 6.3%) than those stented (11.1% ± 3.6%) ($p < 0.0001$). Figures 4 and 5 illustrate the presence of GFP+ cells in coiled and stented aneurysms, respectively, and Supplementary Table II shows the proportion of GFP+ cells for all aneurysms in each ROI.

Histology and Immunostaining

Stent-treated aneurysms demonstrated significantly superior histological neointima formation compared with coiled aneurysms ($p = 0.002$ for vital and $p = 0.009$ for decellularized aneurysms). Immunohistology revealed the presence of smooth muscle actin-expressing cells along the neointima and inside the scarred aneurysm sac in healed aneurysms of either treatment modality. Furthermore, the innermost layer of the neointima was lined by flat Von Willebrand factor expressing endothelial cells (Figure 6). An endothelial lining was also detected along coil's

surface inside the thrombus. Despite better healing, stent-treated animals showed higher grades of local inflammatory cells. Compared with decellularized coiled aneurysms, decellularized aneurysms were characterized by significantly more inflammation in their wall ($p = 0.0036$) and periadventitia ($p = 0.0026$), and greater periadventitional fibrosis ($p = 0.018$). Furthermore, compared with vital aneurysms after stent treatment, decellularized aneurysms after stent treatment showed also pronounced inflammatory cells in the aneurysm wall ($p < 0.001$) and adventitia tissue layer ($p < 0.001$). Detailed histological analysis is given in the Supplemental Figure III.

Discussion

Results demonstrated that treatment with stents achieved superior healing to coiling at 3- to 28-day follow up in this rat saccular aneurysm model. Coiled aneurysms often exhibited insufficient neointima formation and thrombus remodeling whereas stented aneurysms showed a clear pattern of early and continuous neointima formation along the stent's surface and simultaneously better intraluminal thrombus organization. Thrombus organizing cells originated predominantly in the adjacent vessel, with a minor contribution of cells originating in the aneurysm wall, for either form of EVT. In particular, the neointima was predominantly formed by cell migration from the adjacent vessel with an ancillary contribution from cells originating in the aneurysm wall. Therefore, the proportion of neointima-forming cells that originated in the aneurysm wall was higher in coiled aneurysms than in stented aneurysms where cells originating in the adjacent vessel may migrate more easily along the scaffold.

Pattern of Aneurysm Healing after EVT

The biological concept of coiling for aneurysm treatment is to introduce intra-aneurysmal thrombus. In successful (complete) aneurysm healing, this unorganized intraluminal hematoma will then transform into granulation tissue that matures into organized fibrosis.[3] Human (and preclinical) histopathological studies revealed a growth pattern that begins at the aneurysm wall, and continues by centripetal expansion of the endothelial cell lining over the granulation tissue toward the center of the aneurysm neck.[3, 5, 20] Light microscopic sequencing over subsequent stadia of aneurysm healing from our study confirmed a clear pattern of healing from the periphery toward the center of the aneurysm and from the base toward its dome. Thereby, the neointima grows progressively thicker over time, with the residual unorganized hematoma being continuously isolated. On the other hand, coiled aneurysms with degenerated, acellular vessel walls in particular showed insufficient thrombus organization and lack of a continuous neointima. This aligns with previous studies that have shown a rarefication of mural cells leading to chronic inflammation, insufficient healing, and eventually aneurysm regrowth und rupture.[5, 7]

Origin of Thrombus-Organizing Cells

Endothelial cells and SMCs, which organize the thrombus, secrete matrix, and build the neointima, may potentially be derived from the aneurysm wall, parent artery, or circulating precursor cells.[12, 21] However, the existence of bone-marrow-derived, circulating progenitor cells remains disputed[14, 22] based on evidence from previous studies showing that these cells play only a minor role in aneurysm healing, if at all.[11, 12, 22] Our study aim to investigate the origin of the principal portion of thrombus-organizing cells would thereby differentiate between the aneurysm wall and parent artery wall as origin for the migrating cells. To determine the true contribution of cells originating in the aneurysm wall, the proportion of about 20% of GFP+ cells in the thrombus of GFP+ aneurysms on wild-type parent arteries after either coil or treatment must be

doubled because that tissue expresses GFP in a mosaic pattern, which thus consists of about half of all cells.

We hypothesized that the contribution of cells originating from the aneurysm wall was smaller than what was found in this experimental setting because the GFP+ experimental aneurysms were made from healthy, cell-rich tissue. In patients, aneurysms may often have a diseased wall with a rarefication of mural cells.[3, 4, 6] Consequently, the pool of cells that can divide and migrate into the thrombus is smaller and the proportion of these cells will diminish. We believe this explains inferior healing of the decellularized aneurysms when compared with the vital ones. Furthermore, this theory is supported by the findings of previous studies that reported on successful direct intra-aneurysmal transplantation of SMC[8] or even unspecific intravascular endografting of mesenchymal stem cells for aneurysm treatment.[23]

Better Neointima Formation along a Scaffold Yields Better Aneurysm Healing

Treatment modality was more impactful for cells in the neointima than in the thrombus. There were significantly more GFP+ cells in the neointima of coiled aneurysms or, conversely, the proportion of cells originating in the parent artery was higher in stented aneurysms. On the basis of this finding and the pattern described above, we concluded that the stent acts as a scaffold for migrating cells from the parent artery. The stent provides a surface onto which the cells attach and differentiate into a secretory or contractile type[3]; without this surface, they continue to migrate toward the inside of the aneurysm sac.[24, 25] This process of endothelialization on the level of the stent results in complete aneurysm healing without residual perfusion. In a previous study on flow-diverter treatment of experimental aneurysms in rabbits, Kadirvel et al. even suggested that endothelialization of the flow diverter is more important than thrombus formation in the aneurysm cavity.[22] In contrast, with coil treatment alone, cells migrate

centripetally from the aneurysm wall toward the center of the aneurysm sac, which leaves a basal central bulge, that results in central residual aneurysm perfusion. This phenomenon may be one of the crucial reasons why the >30% rate of residual perfusion/recurrence after coiling decreased to <5% recurrence after stent-assisted coiling. [1, 2, 26]

Endothelialization of Neointima, Stent, and Coils

The outermost layer of the neointima is the endothelium, a biologically active single layer of cells, that ensures a living, non-thrombogenic surface toward the lumen of the parent artery.[27] Immunohistological staining in our specimens confirmed the presence of endothelialization along the neointima and also around coils and stent hardware. Thus, in aneurysms with recurrence, endothelial cells occurred in a monolayer around the residually perfused clefts, which extended from the parent artery inside the scarred former aneurysm dome. This finding aligns with Raymond et al. who studied endothelialization in a venous pouch canine aneurysm model treated with embolic agents. The authors found slit-like endothelialized spaces between the wall of the aneurysm and the embolic agent, which remained connected to the parent artery; they concluded these endothelialized clefts to be the reason for persistence of residual lesions and of aneurysmal recanalization after embolization.[25, 27]

With stent treatment, the growth of a rectilinear endothelial cell layer along the scaffold is facilitated as the stent acts protectively to avoid endothelialized extension inside the aneurysm. Furthermore, in the one case of our series with persistent residual perfusion after stent treatment, an endothelialized cavern below the stent was visible. In studies investigating flow diverter treatment for experimental aneurysms in rabbits, researchers found circumferential complete apposition of the device on the parent artery wall to be the crucial point for successful aneurysm occlusion with that treatment.[28, 29]

In another study on endothelial lining after stent treatment in experimental aneurysms in dogs, Soulez et al. suggested that endothelial denudation of the aneurysm as a potential new therapeutic strategy to improve long-term results after stent treatment.[30] On the basis of our results, we conclude that formation of a non-interrupted, continuous endothelium is fundamental for aneurysm healing whereas excessive endothelium formation extending inside the aneurysm may promote incomplete healing, which is associated with residual perfusion and recurrence. An endovascular scaffold may help to guide premature endothelium along the desired level, thereby promoting subendothelial deposition of fibrous matrix and SMC. Without a supportive scaffold, the endothelial lining around coils may be more prone to connect directly with the endothelial cells at the aneurysmal neck, thereby forming endothelialized clefts that will lead to incomplete healing and residual perfusion.

Strengths and Limitations

A recent study performed in the same aneurysm model used in our experiments showed that aneurysm growth, intraluminal thrombus resolution, and wall inflammation were influenced by sex hormones.[31] Therefore, our study used only male rats to avoid confounding effects by estrogen and androgen hormones. Second, in our experimental setting that combined a GFP+ graft aneurysm on a wild-type recipient parent artery (or vice versa), GFP signal allowed us to track with certitude the origin of all GFP+ cells (to either the donor or recipient). However, it does not work conversely: GFP+ animals are hybrids with GFP expression in a mosaic pattern. Accordingly, a GFP-negative cell may originate from the wild-type animal or from the mutant rat, and it is not possible to visualize that difference. With our main focus on the role of cells of the aneurysm wall, we did not use any marker to differentiate between cells derived from circulating cells in the blood stream and those derived from true migration of neighboring cells.

Future experiments would offer great interest by labeling a specific area (e.g., parent artery) in the recipient animal. Furthermore, the circumjacent physiological milieu in a rat extracranial space differs from that in human subarachnoid space. Although the coils used are well established for treatment of human cerebral aneurysms, the stents were balloon-mounted, specifically shortened for suitability in rats, and are not routinely used in a clinical setting. Therefore, histological findings of this proof-of-concept study should be cautiously extrapolated to humans. Lastly, in the model used, hemodynamic characteristics and subsequent biological processes (e.g., rate of spontaneous thrombosis, aneurysm healing) are relevantly influenced by the side wall constellation of the aneurysm.[32] Despite all efforts made to randomize animals and to standardize surgical procedures and aneurysm dimensions upon creation, we cannot completely exclude differences in hemodynamics between groups.

Conclusions

In a rat saccular sidewall model, aneurysm healing after EVT depends on cell migration from the parent artery and from the aneurysm wall. For thrombus organization, cell migration from the parent artery seems to be quantitatively predominant over migration from the aneurysm wall after either coil or stent treatment. However, neointima formation in coiled aneurysms relies more on cell migration from the aneurysm wall whereas the contributions of cells originating in the parent artery is higher in stent-treated aneurysms. Therefore, continuous endothelial lining along the parent artery's lumen, which is facilitated by an endovascular scaffold, may be a decisive factor for complete aneurysm healing after EVT. In terms of translation into clinical practice, these findings may explain the variability in achieving complete aneurysm healing after coil treatment and the improved healing rate in stent-assisted coiling compared with coiling alone.

Acknowledgements: We acknowledge Prof. Rainer Grobholz for his support with digital histology. We also thank Prof. E. Kobayashi for allowing us to freely use his transgenic Lewis rat strain. Furthermore, we are thankful Mary Kemper for editing. Finally, we thank Carline Perren for her help with regulatory and administrative tasks.

Funding: This work was supported by research funds of the Research Council, Kantonsspital Aarau, Aarau, Switzerland (FR 1400.000.054). Dr. Serge Marbacher reports a grant from Swiss National Science Foundation (310030_182450). Stents shortened for rat-specific application were supplied by Biotronik AG, Centre for Vascular Intervention, Bülach, Switzerland. The authors are solely responsible for the design and conduct of the presented study and declare no competing interests.

Disclosures: The authors declare no relevant conflict of interest.

Online supplemental materials: Please see https://www.ahajournals.org/journal/str for expanded Materials & Methods, online Tables I-II and online Figures I – III.

References

1. Raymond J, Guilbert F, Weill A, Georganos SA, Juravsky L, Lambert A, Lamoureux J, Chagnon M, Roy D. Long-term angiographic recurrences after selective endovascular treatment of aneurysms with detachable coils. *Stroke*. 2003;34:1398-1403
2. Songsaeng D, Geibprasert S, ter Brugge KG, Willinsky R, Tymianski M, Krings T. Impact of individual intracranial arterial aneurysm morphology on initial obliteration and recurrence rates of endovascular treatments: A multivariate analysis. *J Neurosurg*. 2011;114:994-1002

3. Marbacher S, Niemela M, Hernesniemi J, Frosen J. Recurrence of endovascularly and microsurgically treated intracranial aneurysms-review of the putative role of aneurysm wall biology. *Neurosurg Rev*. 2017
4. Frosen J. Smooth muscle cells and the formation, degeneration, and rupture of saccular intracranial aneurysm wall--a review of current pathophysiological knowledge. *Transl Stroke Res*. 2014;5:347-356
5. Nevzati E, Rey J, Coluccia D, Gruter BE, Wanderer S, vonGunten M, Remonda L, Frosen J, Widmer HR, Fandino J, et al. Aneurysm wall cellularity affects healing after coil embolization: Assessment in a rat saccular aneurysm model. *J Neurointerv Surg*. 2019
6. Marbacher S, Marjamaa J, Bradacova K, von Gunten M, Honkanen P, Abo-Ramadan U, Hernesniemi J, Niemela M, Frosen J. Loss of mural cells leads to wall degeneration, aneurysm growth, and eventual rupture in a rat aneurysm model. *Stroke*. 2014;45:248-254
7. Frosen J, Piippo A, Paetau A, Kangasniemi M, Niemela M, Hernesniemi J, Jaaskelainen J. Remodeling of saccular cerebral artery aneurysm wall is associated with rupture: Histological analysis of 24 unruptured and 42 ruptured cases. *Stroke*. 2004;35:2287-2293
8. Marbacher S, Frosen J, Marjamaa J, Anisimov A, Honkanen P, von Gunten M, Abo-Ramadan U, Hernesniemi J, Niemela M. Intraluminal cell transplantation prevents growth and rupture in a model of rupture-prone saccular aneurysms. *Stroke*. 2014;45:3684-3690
9. Adibi A, Eesa M, Wong JH, Sen A, Mitha AP. Combined endovascular coiling and intra-aneurysmal allogeneic mesenchymal stromal cell therapy for intracranial aneurysms in a rabbit model: A proof-of-concept study. *J Neurointerv Surg*. 2017;9:707-712
10. Kuwabara A, Liu J, Kamio Y, Liu A, Lawton MT, Lee JW, Hashimoto T. Protective effect of mesenchymal stem cells against the development of intracranial aneurysm rupture in mice. *Neurosurgery*. 2017;81:1021-1028

11. Frosen J, Marjamaa J, Myllarniemi M, Abo-Ramadan U, Tulamo R, Niemela M, Hernesniemi J, Jaaskelainen J. Contribution of mural and bone marrow-derived neointimal cells to thrombus organization and wall remodeling in a microsurgical murine saccular aneurysm model. *Neurosurgery*. 2006;58:936-944; discussion 936-944
12. Fang X, Zhao R, Wang K, Li Z, Yang P, Huang Q, Xu Y, Hong B, Liu J. Bone marrow-derived endothelial progenitor cells are involved in aneurysm repair in rabbits. *J Clin Neurosci*. 2012;19:1283-1286
13. Hoh BL, Velat GJ, Wilmer EN, Hosaka K, Fisher RC, Scott EW. A novel murine elastase saccular aneurysm model for studying bone marrow progenitor-derived cell-mediated processes in aneurysm formation. *Neurosurgery*. 2010;66:544-550; discussion 550
14. Li ZF, Fang XG, Yang PF, Huang QH, Zhao WY, Liang C, Zhao R, Liu JM. Endothelial progenitor cells contribute to neointima formation in rabbit elastase-induced aneurysm after flow diverter treatment. *CNS Neurosci Ther*. 2013;19:352-357
15. Kilkenny C, Browne WJ, Cuthill IC, Emerson M, Altman DG. Improving bioscience research reporting: The arrive guidelines for reporting animal research. *PLoS Biology*. 2010;8:e1000412
16. Inoue H, Ohsawa I, Murakami T, Kimura A, Hakamata Y, Sato Y, Kaneko T, Takahashi M, Okada T, Ozawa K, et al. Development of new inbred transgenic strains of rats with lacz or gfp. *Biochem Biophys Res Commun*. 2005;329:288-295
17. Marbacher S, Marjamaa J, Abdelhameed E, Hernesniemi J, Niemela M, Frosen J. The helsinki rat microsurgical sidewall aneurysm model. *J Vis Exp*. 2014:e51071
18. Nevzati E, Rey J, Coluccia D, D'Alonzo D, Gruter B, Remonda L, Fandino J, Marbacher S. Biodegradable magnesium stent treatment of saccular aneurysms in a rat model - introduction of the surgical technique. *J Vis Exp*. 2017

19. Gruter BE, Taschler D, Rey J, Strange F, Nevzati E, Fandino J, Marbacher S, Coluccia D. Fluorescence video angiography for evaluation of dynamic perfusion status in an aneurysm preclinical experimental setting. *Oper Neurosurg (Hagerstown)*. 2019
20. Bavinzski G, Talazoglu V, Killer M, Richling B, Gruber A, Gross CE, Plenk H, Jr. Gross and microscopic histopathological findings in aneurysms of the human brain treated with guglielmi detachable coils. *J Neurosurg*. 1999;91:284-293
21. Asahara T, Murohara T, Sullivan A, Silver M, van der Zee R, Li T, Witzenbichler B, Schatteman G, Isner JM. Isolation of putative progenitor endothelial cells for angiogenesis. *Science*. 1997;275:964-967
22. Kadirvel R, Ding YH, Dai D, Rezek I, Lewis DA, Kallmes DF. Cellular mechanisms of aneurysm occlusion after treatment with a flow diverter. *Radiology*. 2014;270:394-399
23. Rouchaud A, Journe C, Louedec L, Ollivier V, Derkaoui M, Michel JB, Mazighi M. Autologous mesenchymal stem cell endografting in experimental cerebrovascular aneurysms. *Neuroradiology*. 2013;55:741-749
24. Marosfoi M, Langan ET, Strittmatter L, van der Marel K, Vedantham S, Arends J, Lylyk IR, Loganathan S, Hendricks GM, Szikora I, et al. In situ tissue engineering: Endothelial growth patterns as a function of flow diverter design. *J Neurointerv Surg*. 2017;9:994-998
25. Raymond J, Darsaut T, Salazkin I, Gevry G, Bouzeghrane F. Mechanisms of occlusion and recanalization in canine carotid bifurcation aneurysms embolized with platinum coils: An alternative concept. *AJNR Am J Neuroradiol*. 2008;29:745-752
26. Zhang X, Zuo Q, Tang H, Xue G, Yang P, Zhao R, Li Q, Fang Y, Xu Y, Hong B, et al. Stent assisted coiling versus non-stent assisted coiling for the management of ruptured intracranial aneurysms: A meta-analysis and systematic review. *J Neurointerv Surg*. 2019;11:489-496

27. Raymond J, Sauvageau E, Salazkin I, Ribourtout E, Gevry G, Desfaits AC. Role of the endothelial lining in persistence of residual lesions and growth of recurrences after endovascular treatment of experimental aneurysms. *Stroke*. 2002;33:850-855

28. Rouchaud A, Ramana C, Brinjikji W, Ding YH, Dai D, Gunderson T, Cebral J, Kallmes DF, Kadirvel R. Wall apposition is a key factor for aneurysm occlusion after flow diversion: A histologic evaluation in 41 rabbits. *AJNR Am J Neuroradiol*. 2016;37:2087-2091

29. King RM, Brooks OW, Langan ET, Caroff J, Clarencon F, Tamura T, Wainwright JM, Gounis MJ, Marosfoi M, Puri AS. Communicating malapposition of flow diverters assessed with optical coherence tomography correlates with delayed aneurysm occlusion. *J Neurointerv Surg*. 2018;10:693-697

30. Soulez G, Lerouge S, Darsaut T, Salazkin I, Oliva VL, Raymond J. Role of the endothelial lining in endoleak formation and persistence after endovascular repair of aneurysm. *J Vasc Interv Radiol*. 2008;19:1070-1078

31. Morel S, Karol A, Graf V, Pelli G, Richter H, Sutter E, Braunersreuther V, Frosen J, Bijlenga P, Kwak BR, et al. Sex-related differences in wall remodeling and intraluminal thrombus resolution in a rat saccular aneurysm model. *J Neurosurg*. 2019:1-14

32. Marbacher S, Wanderer S, Strange F, Gruter BE, Fandino J. Saccular aneurysm models featuring growth and rupture: A systematic review. *Brain Sci*. 2020;10

Figure legends:

Figure 1: Experimental setting and groups

Wilde type aneurysms were sutured on green fluorescent protein expressing (GFP+) mutants and endovascularly treated with either stent or coils. Likewise, GFP+ aneurysms were sutured on wild type receiver animals and received stent or coil treatment. Reasons for early dropouts were anesthesia overdosage during induction* and aneurysm growth and rupture 7 days after coiling and hemiparesis due to subacute aortic thrombosis 7 days after coiling**.

Figure 2: Timely evolution of aneurysm healing

Sagittal cross-sections of a healing aneurysm with stent treatment (arrows point at exemplary stent artifacts; * indicates parent artery's lumen). Masson's trichrome staining depicts blood in red and collagen fibers in green. Already after 3 days (A) a small neointima is formed (between arrowheads). Over the following weeks (7 days in (B) and 14 days in (C)), a pattern of progressive neointima formation from the periphery towards the center and from the basis of the aneurysm into the direction of the dome is visible. Simultaneously the intraluminal hematoma (#) is gradually organized into mature thrombus (arrowheads in (C)) and finally into scar tissue. After 28 days (D), this aneurysm has nearly healed: note thick layer of fibrotic tissue with some minor thrombus in organization (†) in the centere and some minor residual hematoma on the very top (#). For further evaluation (please see Figures 4 and 5), regions of interest were defined in the aneurysm wall (a), in the intraluminal thrombus (b) and in the neointima (c). Digitalized histology, magnification indicated by scale bar.

Figure 3: Comparison of cell count in different ROIs between coil and stent treated aneurysms

Graph shows relative cell counts for GFP positive aneurysms sutured on wild type animals and treated with either coil or stent. Comparison between treatments revealed no difference with regard to the proportion of GFP positive cells in the aneurysm wall (49.2 %, in coil vs 48.7 % in stent treatment $p = 0.37$), neither in the intraluminal thrombus (20.5 % in coil vs 20.3 %, in stent $p = 0.94$), but significant difference in the neointima (31.6 % in coil vs 8.4 % in stent treatment, **: $p = 0.0001$).

Figure 4: Illustrative panel of GFP-signal in a GFP positive aneurysm on wild type parent artery and coil treatment

Overview (A) of DAPI staining (blue) and GFP-Filter (green) merged images of a GFP positive aneurysm on a wild type parent artery after 28 days of coil treatment (# indicates coil artefact). An exemplary magnified cut-out of the aneurysm wall (B) reveals high GFP cellularity (approximately 50 %). Inside the intraluminal thrombus (C) approximately 20 % of cells are GFP positive (arrows). However, in the neointima (D) approximately 30 % of all show a positive GFP signal (arrows). The parent artery's lumen is marked with an asterisk (*). Digitalized histology, magnification indicated by scale bars.

Figure 5: Illustrative panel of GFP-signal in a GFP positive aneurysm on wild type parent artery and stent treatment

Overview (A) of DAPI staining (blue) and GFP-Filter (green) merged images of a GFP positive aneurysm on a wild type parent artery after 28 days of stent treatment (# indicates stent artefact). An exemplary magnified cut-out of the aneurysm wall (B) shows high GFP cellularity

(approximately 50 %). Inside the intraluminal thrombus (C) approximately 20 % of cells are GFP positive (arrows), whereas in the neointima (D) GFP positive cells are much rarer, around 10 % (arrows). The parent artery's lumen is marked with an asterisk (*). Digitalized histology, magnification indicated by scale bars.

Figure 6: Cell types in thrombus and neointima

Hemalaun-eosinophil staining (A and D) and immuno-staining for smooth muscle actin (B and E) and vonWillebrand-Factor (C and F) in a coiled aneurysm (top row) and in a stent-treated aneurysm (bottom row) after 28 days. The lumen of the parent artery is marked with an asterisk (*). Note the incomplete healing status with central residual aneurysm perfusion in the coiled aneurysm (arrow in A). Removal of coils during histological processing leaves artefact in the thrombus (#) and an iatrogenic discontinuation of the neointima (arrow heads). Likewise, stent artefacts (†) are visible in panel D, E and F. The brown signal in (B) along the vessel wall of the parent artery but also in the neointima and inside the thrombus indicates the presence of smooth muscle actin expressing cells, such as myofibroblasts and myoblasts. The pattern of distribution in E suggests migration from the bottom (neointima/stent) towards the top of the aneurysm dome. The brown cells in (C) and (F) represent endothelial cells (arrows), confirming endothelialisation along the neointima and around coils (not shown) and stent loops (F). Digitalized histology, magnification indicated by scale bars.

Supplementary Materials

Supplementary Methods

Anesthesia protocol for the replication cohorts

Despite low morbidity and mortality related to anesthesia, a periodic veterinary revision of all standard procedures in our lab led to an amended rat anesthesia protocol between the operations conducted in the initial main experiments and later replication cohort. Therefore, the revised anesthesia protocol was as follows: Rats were anesthetized with a mix of Fentanyl (0.005 mg/kg; Sintetica, S.A. Switzerland) + Medetomidine (0.15 mg/kg; Vibrac, Switzerland) + Midazolam (2 mg/kg; Roche, Switzerland) administrated in one single injection subcutaneously. Thereafter, they were placed in a clean box and O_2 was provided until loss of consciousness. For prolonged anesthesia exceeding 45 minutes, continuous Isoflurane (1.0 - 2.0 % titrated to effect in 100% O_2) was administered via face mask. At the end of the surgery, anesthesia was reversed with a mix of Buprenorphine (0.05 mg/kg; Indivior, Switzerland) + Atipamezol (0.75 mg/kg; Arovet AG, Switzerland) + flumazenil (0.2 mg/kg; Labatec-Pharma, Switzerland) subcutaneously; Meloxicam (1 mg/kg; Boehringer Ingelheim, Switzerland) was given subcutaneously for continuous analgesia. Postoperatively, Meloxicam (1 mg/kg; Boehringer Ingelheim, Switzerland) and Buprenorphine (0.05 mg/kg; Indivior, Switzerland) was administered four times a day subcutaneously for 3 days. For the first night, buprenorphine was provided in drinking water (6 ml Temgesic (Buprenorphine 0.3 mg/ml) + 360 ml drinking water +10 ml Glucose 5%).

GFP staining protocol

As autofluorescence did not always reveal a strong enough signal for digitalization and further post-processing, these slides were stained with an antibody specific to green-fluorescent protein, linked to a secondary antibody with a stronger fluorescent marker. Detailed straining protocol started with deparaffinization: Xylol bath for 10 min was followed by a descending ethanol dilution (100%, 95%, 80%, 70%, and 35%) for 5 min each and finally in distilled water for 20 min. Thereafter, slides were washed in PBS and boiled in a microwave (4 min at 350 W) with a pH-titrated citrate buffer to pH 6.0 (2.94 g

tri-Na-Citrat-Dihydrat, 1 liter distilled water, 500 µl hydrochloric acid). After slides were boiled in the microwave (4 min at 350 W) with a visual control after 3 minutes to re-add citrate buffer if needed, they were defrosted in the microwave for 4 min, left to cool for 30 minutes, and re-washed in PBS. Next, 9 ml PBS-Triton 0.1% + 1 ml horse serum were added and incubated for 45 min. After washing in PBS again, slides were incubated at 4°C for approximately 12 hours with a solution of 5 ml PBS + 5 ml PBS-Triton 0.1% of which 500 µl was discarded and replaced by 500 µl horse serum. Additionally, 32 µl rabbit anti-GFP cell signaling antibody (1:250) was added. Slides were then washed again in PBS. The final step, performed light protected, had slides incubated with DAPI + 32 µl Alexa anti-rabbit 594 (1:250) antibody for 2 hours at room temperature before covering with a cover slip and beginning microscopy studies.

Four-Point Histological Grading System (Neointima Score)

Scores were graded as previously reported.[6] Briefly, the following characteristics were assessed and scored as follows: Neointima formation (0 = none, 1 = organizing thrombus, 2 = organizing thrombus and neointima formation, 3 = mature neointima); Neutrophils in the thrombus (0 = none, 1 = mild, 2 = moderate, 3 = severe); Aneurysm wall inflammation (0 = none, 1 = few (1-3 spots), 2 = many (> 4 spots), 3 = ubiquitous); Aneurysm wall cellularity (0 = none, 1 = few (1-3 spots), 2 = many (> 4 spots), 3 = ubiquitous); Periadventitial inflammation thrombus (0 = none, 1 = mild, 2 = moderate, 3 = severe); Periadventitial fibrosis thrombus (0 = none, 1 = mild, 2 = moderate, 3 = severe). Scores were dichotomized (none/mild versus moderate/severe and none/ organizing thrombus versus organizing thrombus and neointima formation/mature neointima).

Supplementary Tables

Supplementary Table I: Aneurysm healing and growth status.

Note that all the stent-treated aneurysms did not show any signs of relevant residual perfusion, whereas incomplete healing was common after coil treatment. Accordingly, decellularized aneurysms with coil treatment showed a tendency to growth.

#	Recipient animal	Aneurysm type	Aneurysm dimensions at creation			Treatment	Follow-up (days)	Relevant residual perfusion	Aneurysm dimensions at follow-up		
			Length	Width	Depth				Length	Width	Depth
1	GFP+ mutant	Decellularized	3.5	3	2	Coil	3	No	3.5	3	2
2	GFP+ mutant	Decellularized	4	2.5	2.5	Coil	3	Yes	4	2.5	2.5
3	GFP+ mutant	Decellularized	4	2.5	2	Coil	7	Yes	4	3	2
4	GFP+ mutant	Decellularized	4	2.5	3	Coil	7	Yes	4	2.5	3
5	GFP+ mutant	Decellularized	4	2.5	2	Coil	14	No	4	2.5	3
6	GFP+ mutant	Decellularized	3.5	3	2.5	Coil	14	Yes	4	2.5	2.5
7	GFP+ mutant	Decellularized	3.5	2	2.5	Coil	21	Yes	3.5	3	4
8	GFP+ mutant	Decellularized	5	3.5	3	Coil	21	No	5	3.5	3
9	GFP+ mutant	Decellularized	4	2.5	3	Coil	28	Yes	4	2.5	3
10	GFP+ mutant	Decellularized	3	3	2	Coil	28	Yes	3.5	2.5	2.5
11	Wilde type	Vital, GFP+	3.5	2.5	3	Coil	3	Yes	4	2	3
12	Wilde type	Vital, GFP+	3	2	2	Coil	3	Yes	3	2	2
13	Wilde type	Vital, GFP+	4	3	2	Coil	7	No	17	7	8
14	Wilde type	Vital, GFP+	3.5	2.5	1.5	Coil	7	No	3.5	2.5	1.5
15	Wilde type	Vital, GFP+	4	3	2	Coil	14	Yes	8	7	6
16	Wilde type	Vital, GFP+	4	3	2.5	Coil	14	Yes	6	2.5	3.5
17	Wilde type	Vital, GFP+	3	2.5	2.5	Coil	21	No	3.5	3.5	3
18	Wilde type	Vital, GFP+	4	2	3	Coil	21	No	3	3	4
19	Wilde type	Vital, GFP+	3.5	2.5	2.5	Coil	28	Yes	8	5	6.5
20	Wilde type	Vital, GFP+	4	3	2	Coil	28	No	5	4	3
21	GFP+ mutant	Decellularized	4.5	2.5	2.5	Stent	3	No	4.5	2.5	2.5
22	GFP+ mutant	Decellularized	4	2.5	2	Stent	3	No	3	4	2.5
23	GFP+ mutant	Decellularized	2.5	2.5	2.5	Stent	7	No	2.5	2.5	2
24	GFP+ mutant	Decellularized	4	2.5	2	Stent	7	No	4	3	2
25	GFP+ mutant	Decellularized	4	3	2	Stent	14	No	4	3	2.5
26	GFP+ mutant	Decellularized	4	2.5	2	Stent	14	No	4.5	3.5	2
27	GFP+ mutant	Decellularized	3	2.5	2	Stent	21	No	3	4	2
28	GFP+ mutant	Decellularized	3	2.5	1.5	Stent	21	Yes	4	4	3

29	GFP+ mutant	Decellularized	4.5	2.5	2	Stent	28	No	3	3	2.5
30	GFP+ mutant	Decellularized	4	2.5	2	Stent	28	No	2.5	3	2.5
31	Wilde type	Vital, GFP+	4	3.5	2	Stent	3	No	4	3.5	2.5
32	Wilde type	Vital, GFP+	4.5	3	1.5	Stent	3	No	4	3	2.5
33	Wilde type	Vital, GFP+	4	3	2	Stent	7	No	4	3.5	2.5
34	Wilde type	Vital, GFP+	4	2	2	Stent	7	No	4	3	2
35	Wilde type	Vital, GFP+	4	3	2.5	Stent	14	No	4	3.5	2.5
36	Wilde type	Vital, GFP+	3	3	2	Stent	14	No	3.5	3	2.5
37	Wilde type	Vital, GFP+	4	3	2.5	Stent	21	No	4.5	3.5	2.5
38	Wilde type	Vital, GFP+	4	3	2.5	Stent	21	No	4	3.5	3.5
39	Wilde type	Vital, GFP+	4	3	2.5	Stent	28	No	4	3	2.5
40	Wilde type	Vital, GFP+	4	3	2	Coil	7	Yes	7.5	4	3
41	Wilde type	Vital, GFP+	4.5	3	1.5	Coil	7	Yes	4.5	4	2.5
42	Wilde type	Vital, GFP+	4	2.5	2	Coil	7	No	7	4	3.5
43	Wilde type	Vital, GFP+	4	3	2.5	Coil	7	No	4.5	4.5	4
44	Wilde type	Vital, GFP+	4	2	2.5	Coil	21	No	4	3.5	3
45	Wilde type	Vital, GFP+	4	2.5	2	Coil	21	No	5.5	3	2.5
46	Wilde type	Vital, GFP+	4.5	2	2.5	Coil	21	Yes	5.5	3.5	3
47	Wilde type	Vital, GFP+	3.5	2.5	2	Coil	21	Yes	7	4.5	5
48	Wilde type	Vital, GFP+	4	2.5	2	Stent	7	No	4	2.5	2
49	Wilde type	Vital, GFP+	4.5	2.5	2	Stent	7	No	4.5	2	2.5
50	Wilde type	Vital, GFP+	4.5	2.5	2	Stent	7	No	4	2.5	2
51	Wilde type	Vital, GFP+	4	1.5	2	Stent	7	No	4	2.5	2
52	Wilde type	Vital, GFP+	4	2.5	2	Stent	21	No	5	5	3.5
53	Wilde type	Vital, GFP+	3	2.5	2	Stent	21	No	4	3	2.5
54	Wilde type	Vital, GFP+	3	1	1.5	Stent	21	No	3	1	1.5

Supplementary Table II: Proportion of GFP positive cells for all aneurysms.

Values for aneurysm wall in decellularized aneurysms. Regard values for thrombus in all animals with 3-day follow-up with caution: these are based on very low absolute numbers (no thrombus organization yet at that early stage and scarcity of cells in decellularized vessels).

#	Recipient animal	Aneurysm type	Treatment	Follow-up (days)	GFP+ aneurysm wall	GFP+ thrombus	GFP+ neointima
1	GFP+ mutant	Decellularized	Coil	3	33.3%	80.7%	81.9%
2	GFP+ mutant	Decellularized	Coil	3	0.0%	34.4%	66.5%
3	GFP+ mutant	Decellularized	Coil	7	50.0%	48.4%	49.1%
4	GFP+ mutant	Decellularized	Coil	7	73.7%	52.7%	48.4%
5	GFP+ mutant	Decellularized	Coil	14	31.6%	65.6%	49.8%
6	GFP+ mutant	Decellularized	Coil	14	50.0%	56.7%	52.7%
7	GFP+ mutant	Decellularized	Coil	21	58.8%	62.3%	1.6%
8	GFP+ mutant	Decellularized	Coil	21	0.0%	32.6%	49.8%
9	GFP+ mutant	Decellularized	Coil	28	17.6%	43.1%	17.0%
10	GFP+ mutant	Decellularized	Coil	28	66.7%	67.2%	51.5%
11	Wilde type	Vital, GFP+	Coil	3	46.3%	43.4%	4.1%
12	Wilde type	Vital, GFP+	Coil	3	63.0%	41.5%	29.2%
13	Wilde type	Vital, GFP+	Coil	7	n/a	n/a	n/a
14	Wilde type	Vital, GFP+	Coil	7	46.2%	11.5%	34.4%
15	Wilde type	Vital, GFP+	Coil	14	62.6%	22.2%	39.0%
16	Wilde type	Vital, GFP+	Coil	14	37.2%	14.9%	48.0%
17	Wilde type	Vital, GFP+	Coil	21	38.4%	35.4%	13.4%
18	Wilde type	Vital, GFP+	Coil	21	42.0%	23.3%	32.3%
19	Wilde type	Vital, GFP+	Coil	28	39.6%	23.4%	21.3%
20	Wilde type	Vital, GFP+	Coil	28	67.2%	13.0%	23.5%
21	GFP+ mutant	Decellularized	Stent	3	46.7%	14.7%	58.7%
22	GFP+ mutant	Decellularized	Stent	3	68.6%	13.1%	50.0%
23	GFP+ mutant	Decellularized	Stent	7	0.0%	54.9%	52.5%
24	GFP+ mutant	Decellularized	Stent	7	35.0%	23.1%	46.3%
25	GFP+ mutant	Decellularized	Stent	14	0.0%	36.8%	68.3%
26	GFP+ mutant	Decellularized	Stent	14	33.3%	38.8%	56.1%
27	GFP+ mutant	Decellularized	Stent	21	21.4%	54.4%	40.8%
28	GFP+ mutant	Decellularized	Stent	21	56.2%	26.0%	33.8%
29	GFP+ mutant	Decellularized	Stent	28	15.4%	45.4%	17.0%
30	GFP+ mutant	Decellularized	Stent	28	89.5%	46.0%	49.1%
31	Wilde type	Vital, GFP+	Stent	3	47.3%	2.0%	0.9%
32	Wilde type	Vital, GFP+	Stent	3	38.3%	1.2%	0.4%
33	Wilde type	Vital, GFP+	Stent	7	67.2%	28.0%	15.5%
34	Wilde type	Vital, GFP+	Stent	7	42.6%	17.1%	7.8%
35	Wilde type	Vital, GFP+	Stent	14	40.7%	14.8%	34.1%
36	Wilde type	Vital, GFP+	Stent	14	50.0%	27.1%	6.6%
37	Wilde type	Vital, GFP+	Stent	21	64.0%	23.2%	12.0%
38	Wilde type	Vital, GFP+	Stent	21	47.0%	13.0%	11.9%
39	Wilde type	Vital, GFP+	Stent	28	40.9%	18.6%	4.0%
40	Wilde type	Vital, GFP+	Coil	7	56.8%	35.6%	30.7%
41	Wilde type	Vital, GFP+	Coil	7	42.6%	39.3%	34.7%
42	Wilde type	Vital, GFP+	Coil	7	38.1%	32.9%	n/a
43	Wilde type	Vital, GFP+	Coil	7	38.3%	11.1%	32.3%

44	Wilde type	Vital, GFP+	Coil	21	41.8%	12.0%	31.6%
45	Wilde type	Vital, GFP+	Coil	21	52.0%	29.9%	33.7%
46	Wilde type	Vital, GFP+	Coil	21	46.2%	17.5%	26.0%
47	Wilde type	Vital, GFP+	Coil	21	54.7%	14.0%	14.9%
48	Wilde type	Vital, GFP+	Stent	7	57.0%	27.4%	11.5%
49	Wilde type	Vital, GFP+	Stent	7	41.0%	29.2%	11.4%
50	Wilde type	Vital, GFP+	Stent	7	50.0%	31.3%	7.0%
51	Wilde type	Vital, GFP+	Stent	7	46.7%	20.2%	16.6%
52	Wilde type	Vital, GFP+	Stent	21	46.0%	20.3%	7.5%
53	Wilde type	Vital, GFP+	Stent	21	53.4%	30.2%	7.8%
54	Wilde type	Vital, GFP+	Stent	21	n/a	33.1%	15.6%

Supplementary Figures

Supplementary Figure I: Aneurysm volume.

Aneurysm volume was calculated at baseline (day of surgery) and follow-up using the cylinder formula (V = π × width/2 × depth/2 × length). On average, aneurysm growth was more pronounced during the study period for coiling (18.3 mm^3 ± 5.8 mm^3 at baseline to 32.4 mm^3 ± 18.0 mm^3 at follow-up, p= 0.001) than stenting (16.3 mm^3 ± 5.0 mm^3 at baseline to 23.5 mm^3 ± 12.0 mm^3 at follow up, p=0.008). In the coil treatment group, four statistical outliers with calculated volumes of 123.7 mm^3, 204.2 mm^3, 263.9 mm^3 and 747.7 mm^3 were omitted in the graph.

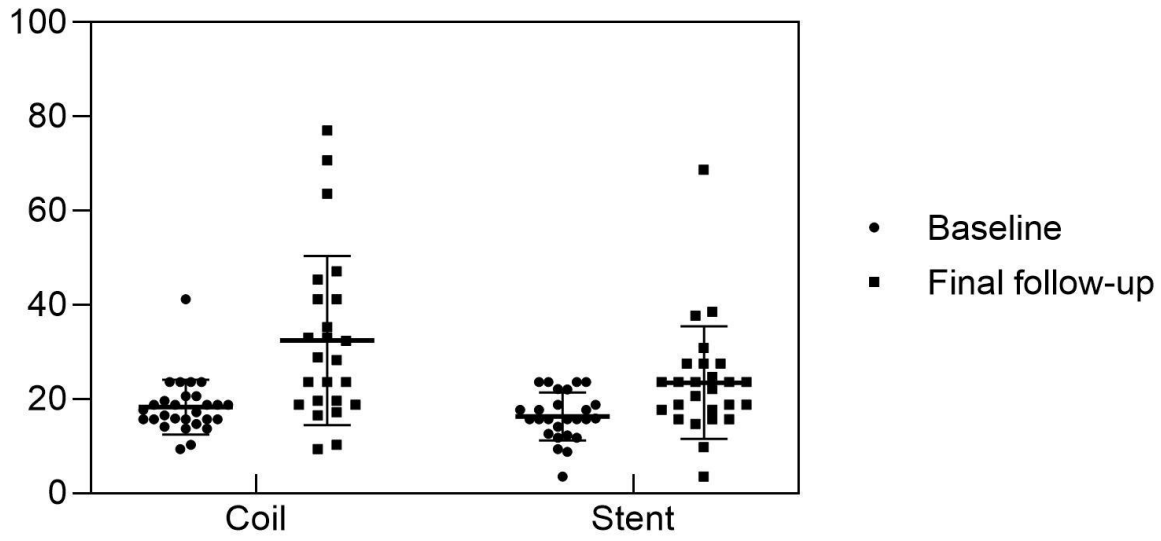

Supplementary Figure II: Surgical details.

No relevant differences between stent and coil treatment groups occurred with respect to body weight or procedural key steps. Operative times with stenting lasted longer than without, necessitating an additional microsurgical suture at the puncture site.

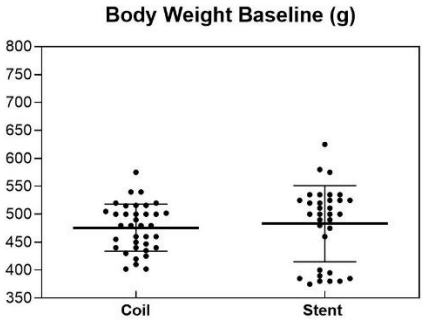
Body Weight Baseline (g)
800
750
700
650
600
550
500
450
400
350
Coil
Stent

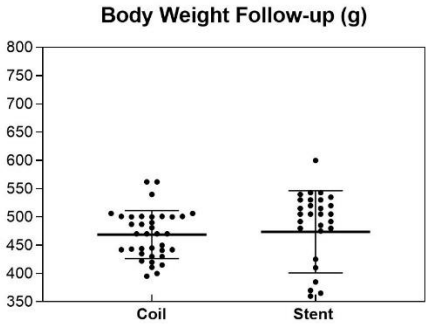
Body Weight Follow-up (g)
800
750
700
650
600
550
500
450
400
350
Coil
Stent

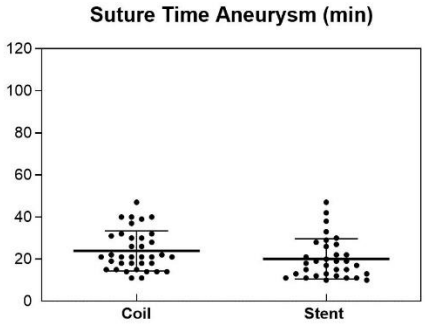
Suture Time Aneurysm (min)
120
100
80
60
40
20
0
Coil
Stent

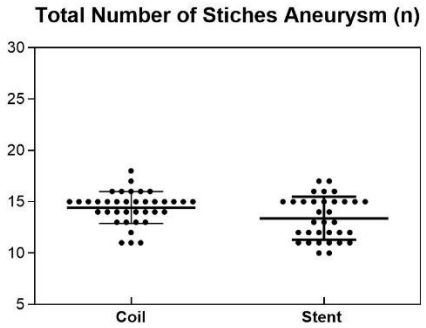
Total Number of Stiches Aneurysm (n)
30
25
20
15
10
5
Coil
Stent

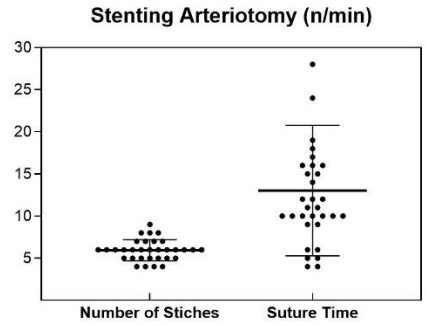
Stenting Arteriotomy (n/min)
30
25
20
15
10
5
Number of Stiches
Suture Time

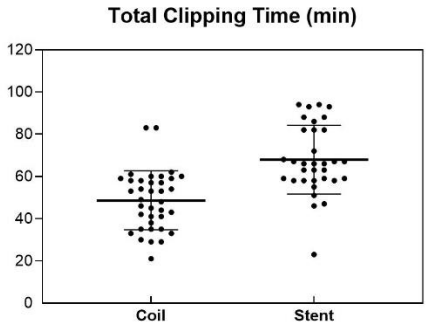
Total Clipping Time (min)
120
100
80
60
40
20
0
Coil
Stent

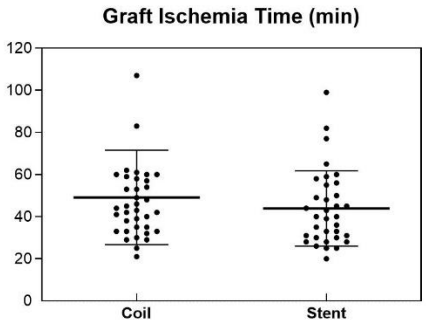
Graft Ischemia Time (min)
120
100
80
60
40
20
0
Coil
Stent

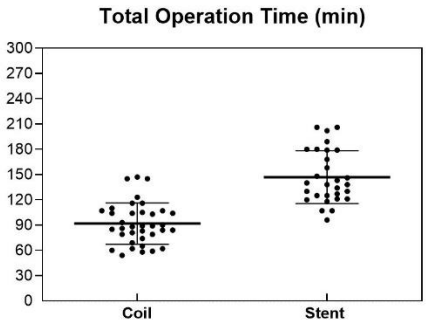
Total Operation Time (min)
300
270
240
210
180
150
120
90
60
30
0
Coil
Stent

Supplementary Figure III: Detailed histological analysis.

Stent-treated aneurysms showed histologically better neointima formation than coil-treated aneurysms but also more pronounced locoregional inflammation, which was most often highest in decellularized stent-treated aneurysms. A 4-point grading system (Neointima-Score) was applied to characterize histology (detailed above in the Supplementary Methods section) as 0 = none, 1 = mild, 2 = moderate, 3 = severe.

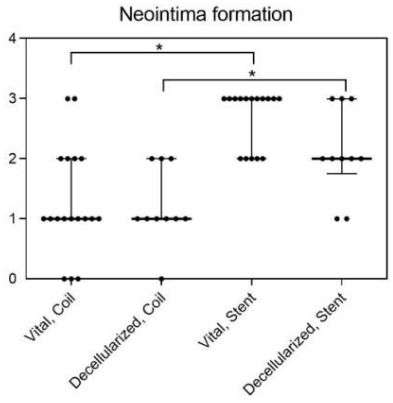
Neointima formation
*
*
4
3
2
1
0
Vital, Coil
Decellularized, Coil
Vital, Stent
Decellularized, Stent

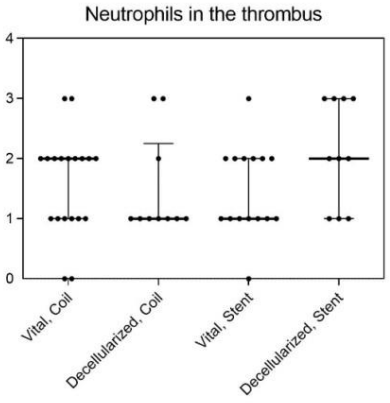
Neutrophils in the thrombus
4
3
2
1
0
Vital, Coil
Decellularized, Coil
Vital, Stent
Decellularized, Stent

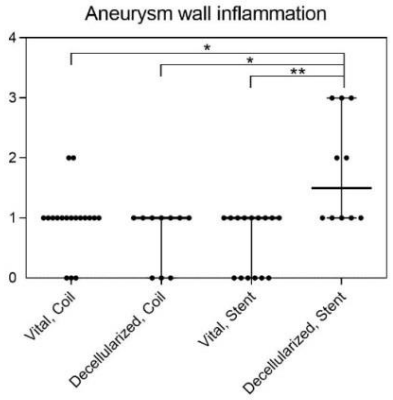
Aneurysm wall inflammation
*
*
**
4
3
2
1
0
Vital, Coil
Decellularized, Coil
Vital, Stent
Decellularized, Stent

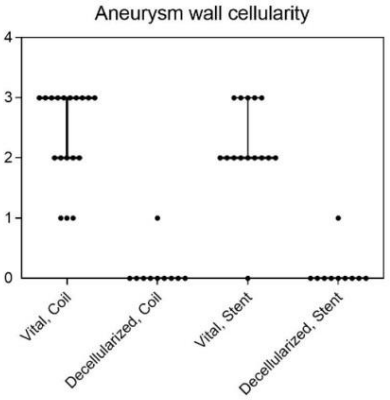
Aneurysm wall cellularity
4
3
2
1
0
Vital, Coil
Decellularized, Coil
Vital, Stent
Decellularized, Stent

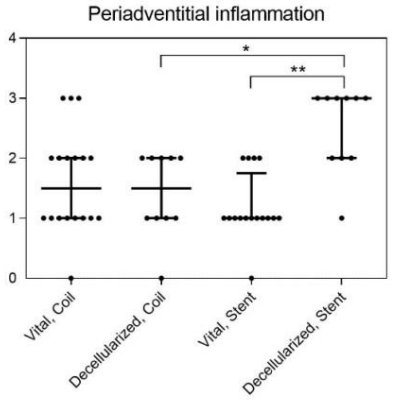
Periadventitial inflammation
*
**
4
3
2
1
0
Vital, Coil
Decellularized, Coil
Vital, Stent
Decellularized, Stent

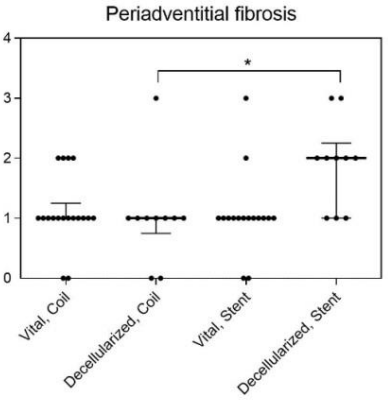
Periadventitial fibrosis
*
4
3
2
1
0
Vital, Coil
Decellularized, Coil
Vital, Stent
Decellularized, Stent